Development of an Adaptable Monitoring Package for Marine Renewable Energy

James Joslin, Northwest National Marine Renewable Energy Center (NNMREC),
University of Washington, Seattle, WA 98195-2600
Edward Celkis, SeaView Systems, Inc., Dexter, MI 48130
Chris Roper, Saab Seaeye, Houston, TX 77084
Andrew Stewart, Applied Physics Laboratory, University of Washington, Seattle, WA 98105
Brian Polagye, NNMREC, University of Washington, Seattle, WA 98195-2600
Email: jbjoslin@u.washington.edu

***Abstract*—The Adaptable Monitoring Package (AMP) along with a Remotely Operated Vehicle (ROV) and custom tool skid, is being developed to support near-field ($\leq$10 meters) and long-range monitoring of hydrokinetic energy converters. The goal for the AMP is to develop a system capable of supporting a wide range of environmental monitoring in harsh oceanographic conditions, at a cost in line with other aspects of technology demonstrations. This paper presents a system description of all related infrastructure for the AMP, including supported instrumentation, deployment ROV and tool skid, launch platform, and docking station. Design requirements are driven by the monitoring instrumentation and the strong waves and currents that typify marine renewable energy sites. Hydrodynamic conditions from the Pacific Marine Energy Centers wave test sites and Admiralty Inlet, Puget Sound, Washington are considered in the design as early adoption case studies. A methodology is presented to increase the capabilities to deploy and operate the AMP in strong currents by augmenting thrust and optimizing the system drag profile through computational fluid dynamic modeling. Preliminary results suggest that the AMP should be deployable in turbulent environments with mean flow velocities up to 1 m/s.**

***Index Terms*—Environmental Monitoring, Hydrokinetics, Remotely Operated Vehicles, CFD**

I. Introduction

Marine renewable energy, including electrical power generation from ocean waves and energetic tidal currents, is advancing towards commercialization. As this occurs, characterizing environmental changes associated with power generation is crucial. Foundational demonstration projects will inform system refinements that allow for sustainable, large-scale implementations. Stressor-receptor interactions with potentially high significance, but broad uncertainties, have been prioritized for study by the research community [1]–[3]. These include dynamic interactions between marine animals and wave or tidal converters (e.g., collision, strike, and evasion), reef effects of converters and their associated support structures, and marine mammal behavioral changes caused by converter sound. The cost to obtain this information must, however, be proportional to the benefit realized and in-line with other project costs. While much of the instrumentation to characterize environmental changes exists, or is in an advanced stage of development, in many cases, the power and data requirements preclude autonomous deployments. Ocean Observing Initiatives [4]–[6] have advanced the infrastructure for cabled observatories in coastal and deep-ocean environments, but the challenge of deploying and maintaining cabled instrumentation at marine energy sites has not received significant attention.

This paper presents an approach to enhance capabilities and reduce costs for environmental data collection around marine renewable energy converters. The system being developed is comprised of an Adaptable Monitoring Package (AMP) that integrates a flexible suite of instrumentation for near-field and long-range observations into a single, streamlined body and a deployment system that allows an inspection-class ROV and custom tool skid to deploy the AMP in the energetic conditions typical of marine energy sites.

The two early-adoption demonstration projects that will deploy this package are the Pacific Marine Energy Centers wave energy test sites (PMEC) off Newport, OR and a tidal energy demonstration project by Public Utility District No. 1 of Snohomish County and OpenHydro, Ltd in Admiralty Inlet, Puget Sound, WA. Hydrodynamic conditions for AMP deployment and operation are based on measured currents at these sites and provide limited windows for instrument maintenance or re-configuration. Maintenance strategies that involve servicing individual instruments (or subcomponents) are precluded. Similarly, water depth and human safety considerations are likely to prohibit the use of divers.

The design philosophy for the AMP centers on a ”plug and socket” architecture whereby the AMP, equipped with a suite of instrumentation, can be rapidly deployed in a precise manner and at low cost. This strategy allows for connection to shore power and data circuits (provided on the device frame), and a recovery process that is simple and inexpensive. Over the lifetime of a project, only the socket remains in the water, with the plug (AMP) readily maintained between deployments on a surface vessel or on shore. This approach to maintaining instrumentation shares a number of commonalities with O&M strategies for wave and tidal current devices,

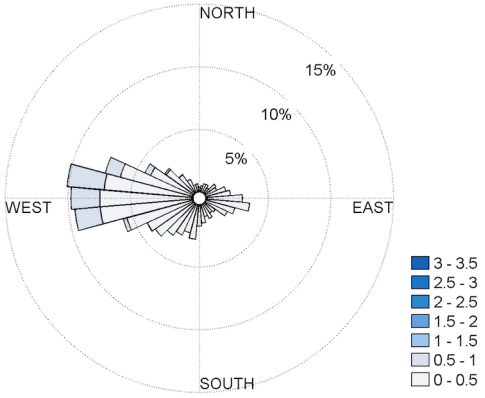

(a) PMEC mean currents (3 m below surface)

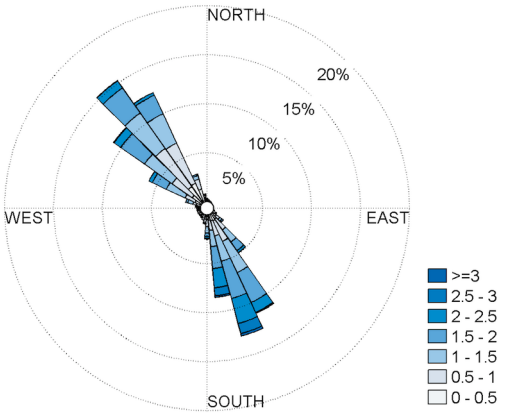

(b) Admiralty Inlet mean currents (10 m above seabed)

Fig. 1: Mean current magnitude and direction for early adopter wave and tidal energy sites

in which the majority of maintenance activities will not be conducted $in-situ$.

The monitoring capabilities supported by the AMP will help researchers study changes to the biological and physical environment associated with harnessing renewable energy from waves and currents.

II. Operating Environments for Marine Renewable Energy Projects

The energetic nature of wave and tidal energy sites presents a challenge for observing the marine environment and conducting in-water operations. Here, we focus on the forces acting on the AMP during deployment and operation due to currents at the Pacific Marine Energy Center's North Energy Test Site (PMEC) and in Admiralty Inlet.

While PMEC serves as a wave energy test site, the site experiences moderate ocean currents and, in general, the forces acting on infrastructure at either a wave or tidal energy site will be a combination of waves and currents. Current data for PMEC consists of a one-month time series obtained from a surface-mounted acoustic Doppler current profiler in the fall of 2012. Current data for Admiralty Inlet consists of a twenty-two month time series obtained from a bottom-mounted acoustic Doppler current profiler between fall 2011 and summer 2013. The magnitude and direction of the mean (non-turbulent) currents at these two locations are shown in Fig. 1 for representative AMP operational depths (3 m below the surface for observations of wave converters at PMEC and 10 m above the seabed for observations of tidal converters in Admiralty Inlet). Mean, sustained currents in Admiralty Inlet exceed 3 m/s (3.5 m/s maximum observed) and approach 1 m/s at PMEC. Consequently, currents in Admiralty Inlet set the maximum loading condition that the AMP would need to sustain. Turbulence intensity in Admiralty Inlet is approximately 10% [7] and, here, we assume that design conditions consist of the AMP being exposed to an exceptionally strong turbulent gust 1.4 times the mean current velocity. This results in a design current of approximately 5 m/s while the AMP is deployed for monitoring on a marine energy converter.

Deploying or recovering the AMP during peak design currents is impractical. However, to be effectively utilized for adaptive management by resource agencies, conditions amenable to recovery and redeployment should occur with relatively high frequency, such as at least one per week. For deployment at a tidal energy site, the AMP would be deployed with the currents fully set in one direction (either on a tide falling towards slack or rising towards peak currents), but with currents less than the operating limit for the ROV-based deployment system. For Admiralty Inlet, if the AMP is able to operate in mean currents of at least 0.7 m/s, the criteria for deployment window frequency can be met. This operating criterion would also allow the AMP to be deployed under most conditions at PMEC.

III. System Description

A. Design Philosophy

To provide real-time monitoring with the anticipated power and data requirements for observations, monitoring packages will need to be connected to shore. While this could be achieved by hard-wiring instrumentation into devices prior to deployment, instrument servicing (which is likely necessary over the lifetime of a converter) would require surface recovery of the entire system. Recovery of a wave converter or tidal turbine to service cabled instrumentation is expensive. Commercial arrays will likely require full system recovery only once in a five-year period, yet instrumentation recovery may occur quarterly over that same period. There is need for an approach that can allow for instrument maintenance and reconfiguration to be performed independently of the converter.

The design philosophy for an adaptable monitoring system with a cabled connection to shore with minimal maintenance costs is the focus of this paper. We present a design that is comprised of two components: 1) the Adaptable Monitoring

Package (AMP) – a flexible package supporting a range of sensors enclosed in a single shrouded body to reduce the system drag in the high current environments, and 2) the Millennium Falcon – the deployment system comprised of a SeaEye Falcon ROV integrated with a customized tool skid.

B. Instrumentation Package (AMP)

The initial instrumentation incorporated into the AMP design is described in Table I with the layout shown in Fig. 2. Most of these instruments, with the exception of the stereo-optical camera system are commercially available. Development and an initial evaluation of the camera system are described in [8]. The leading constraints on the AMP layout are associated with the minimum separation distance between hydrophones in the localizing array and between strobes and the optical cameras. In order to localize marine mammal vocalizations at frequencies of a few kHz, the hydrophone elements require a minimum separation of approximately 1 m in either a tetrahedral or three-dimensional L configuration [9]. Similarly, camera-strobe separation of 1 meter has been shown to reduce backscatter from biological flocculent [8], [10]. Both the optical and acoustical cameras, as well as the acoustic Doppler profiler must also be oriented such that the regions or profiles of interest are within the field of view. The remaining instruments generally require the exposure of a hydrophone element (e.g., C-POD, Vemco receiver) or pump intake (e.g., CTDO) that do not have strict separation or directionality requirements.

C. Deployment System ("Millennium" Falcon)

The Saab Seaeye Falcon is a commercially available inspection-class ROV that weights 60 kg in air and has dimensions of 1 m long by 0.6 m wide by 0.5 m tall (www.seaeye.com/falcon.html). With 4 vectored horizontal thrusters and one vertical thruster, the Falcon is capable of 50 kgf in the forward direction and 13 kgf in the vertical direction. The system is powered and controlled from a deckbox that provides single phase 100-270 VAC at 2.8 kW. Due to the compact size and basic power requirements, the Falcon may be deployed from vessels of opportunity unable to accommodate larger, work class vehicles.

The Millennium tool skid is being developed in cooperation with SeaView Systems and is modeled after the Raptor modification to the Falcon ROV. SeaView Systems Raptor, shown in Fig. 3, is a bolt-on tool skid that provides a second suite of five thrusters to the Falcon for added power, stability and overall capability. This tool skid doubles the thrust of the base ROV while providing 100% redundancy of system propulsion and no interference to the Falcon.

The tool skid works in a Master/Slave configuration with the Falcon‘s surface control unit. Pilot commands are transmitted via a RS485 BUS to all of the vehicles assemblies such as the thrusters, tilt motor, and lamps. At the heart of the Raptor or Millennium is SeaView‘s thruster control board which receives the Falcon commands and emulates them to control the appropriate thrusters on the tool skid. In addition

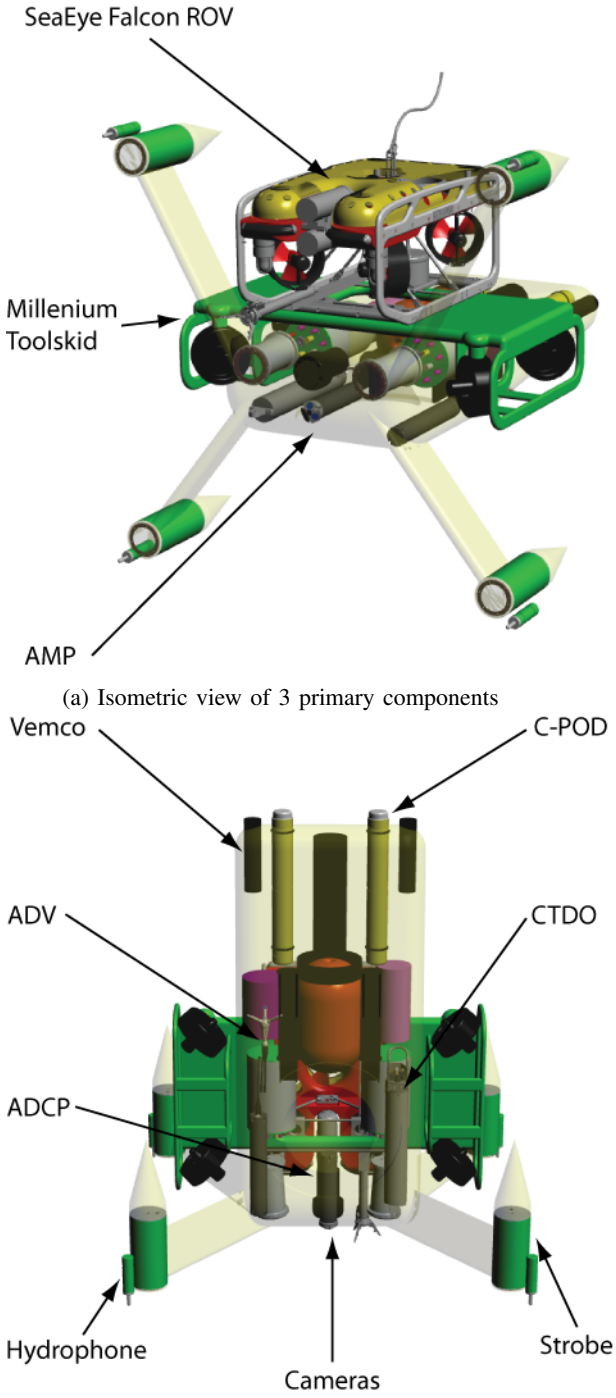

(a) Isometric view of 3 primary components

(b) Bottom view with monitoring instrumentation

Fig. 2: Preliminary design models of the AMP and the Millennium Falcon deployment ROV

TABLE I: Monitoring instrumentation incorporated in the initial AMP design with manufacturer, monitoring capabilities, and size constraints.

Instrument	Manufacturer	Monitoring Capabilities	Layout and Orientation Constraints
Stereo-Optical Camera System	Integrated System – UW Custom, Cameras – Allied Vision Tech., Strobes – Excelitas	Near-field marine animal interactions with turbine with potential for species level identification	0.5 m camera separation, 1 m strobe/camera separation, must face region of interest
Acoustical Camera	BlueView P900-2250	Near-field marine animal detection with capabilities for optical camera triggering	Must face region of interest
Hydrophone Array	OceanSonics iCListen HF	Marine mammal localization and device noise characterization	$\geq$1 m separation between hydrophone elements
Acoustic Doppler current profiler	Nortek Aquadopp 1 MHz	Near-field current profiling to study inflow and wake	Must face towards profile of interest
Acoustic Doppler velocimeter	Nortek Vector	Near-field current point measurement to study inflow and wake turbulence	Sensor head unobstructed
Water quality	SeaBird 16+ v2 CTDO	Water quality and property observations	Unobstructed intake
Cetacean click detector	Chelonia C-POD	Harbor porpoise click detection	Exposed hydrophone element
Fish tag receiver	Vemco VR2W	Tracking of tagged fish	Exposed head

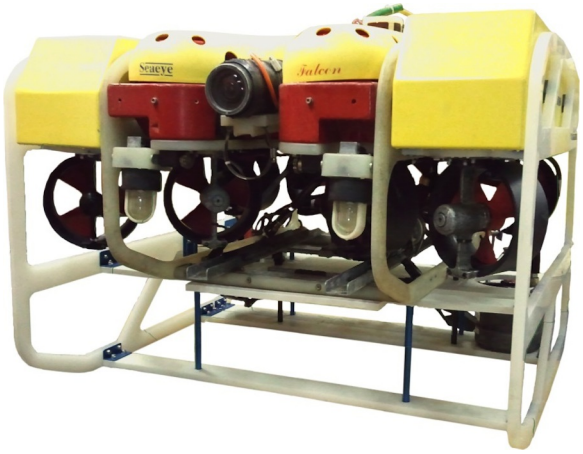

Fig. 3: SeaView System's Raptor ROV tool skid

to the thruster augmentation, the Millennium will incorporate the tooling required to align the AMP with the docking station, engage the mounting clamps, and mate the hybrid connector the wet-mate connector. The Teledyne ODI NRH hybrid electro-optical wet-mate connector has been selected for this mission, given its use in similar applications for ocean observing.

D. Deployment and Recovery Operations

The concept of operations for AMP deployment is structured to minimize the time required to dock the AMP as limited windows are afforded by slack water at tidal energy sites. This operation is illustrated in Fig. 4 for a representative tidal turbine to demonstrate scale. With the Millennium Falcon connected to the AMP, the system would be deployed from a relatively unspecialized vessel.

The Millennium Falcon and AMP would be lowered to the approximate depth of the docking station via a basic garage style launch platform. This is intended to minimize the drag on the ROV umbilical (i.e., the umbilical between the vessel and launch platform will be relieved of strain at the launch platform). The combined system would then be powered up and flown off of the launch platform to a docking station (as shown in Fig. 4on the device. The conical shape of the docking station allows for proper alignment of the wet-mate connector over a range of angular positions. Once alignment is confirmed by a downward-looking camera, a docking clamp will be engaged and the wet-mate connector on the AMP will be plugged into the mating receptacle on the docking platform. Once the AMP instrumentation is brought online, the Millennium Falcon will disengage from the AMP and return to the surface. Both the Millennium Falcon and launch platform will then be recovered by the surface vessel.

Recovery of the AMP from the docking platform will utilize an acoustic release and a tethered float housed within the shrouded body. The release will be triggered from a surface vessel to provide for recovery in the event that shore power or communication with the AMP is interrupted. Once the float is recovered by the surface vessel, the initial tension will (sequentially) disconnect the wet-mate and then release the clamping mechanism, allowing the AMP to be raised to the surface. A similar method has been used for the recovery of Sea Spiders in Admiralty Inlet [11]. In the case of a release malfunction, the Millennium Falcon, or another ROV, could be used to free the float and disengage the clamping mechanism.

IV. System Optimization for Deployment and Operation at Marine Renewable Energy Sites

A. Introduction

Given the strong currents and wave action that the AMP and Millennium Falcon will experience during deployment and operation (Section II), drag profiles should be minimized. To limit non-recurring engineering, the Seaeye Falcon ROV is assumed to have a fixed geometry. During deployments at tidal and wave energy sites, the Millennium Falcon will be required to drive the AMP against moderate currents and maneuver it into position on a docking station. For the purpose of system optimization, the design condition for system deployment was assumed to be a head-on mean relative velocity of 1 m/s with

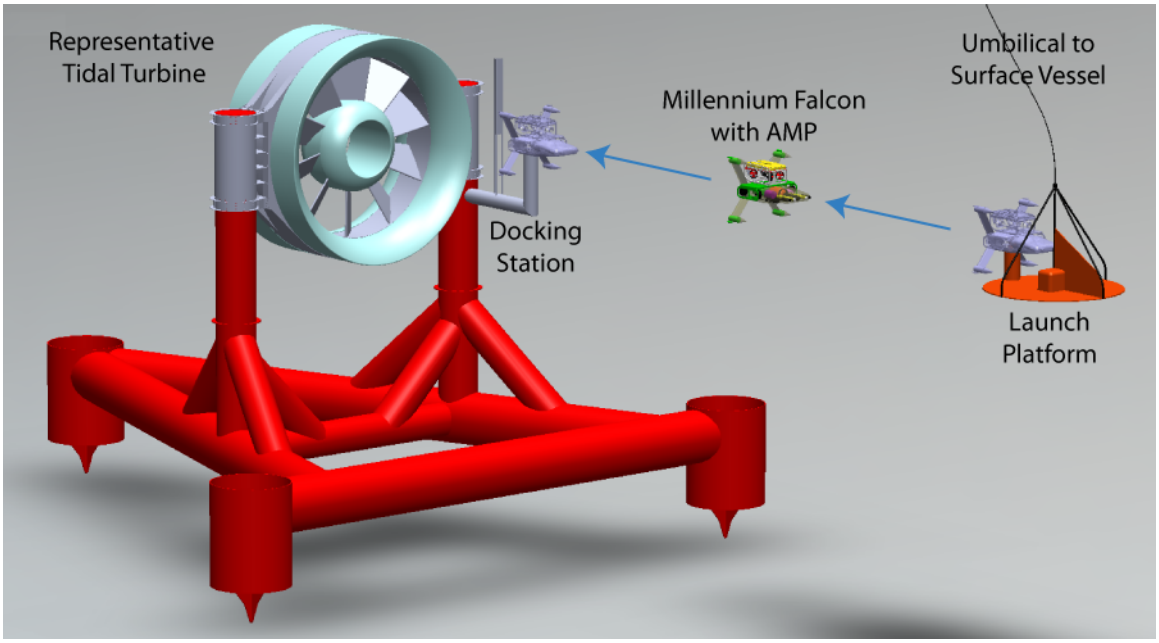

(a) AMP deployment operation from launch platform onto the docking station

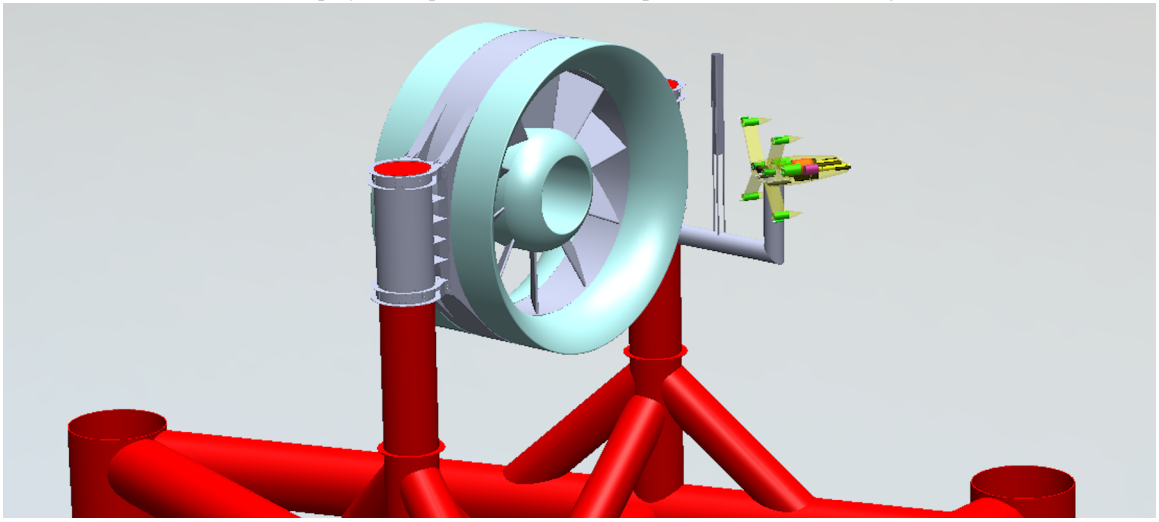

(b) AMP docked in the monitoring position after detachment of the deployment ROV

Fig. 4: Representative AMP deployment for a tidal turbine equipped with a docking station

turbulence intensity of 15% and a 1 m dominant length-scale[1]. For operational monitoring at a tidal energy site, the AMP will be exposed to much stronger currents, with turbulent peaks around 5 m/s. The force of these currents on the AMP body drives the design loads for the docking clamp and the AMP's internal structure.

In general, the profile of the AMP and Millennium Falcon is sufficiently complex to introduce large uncertainties into analytical drag estimates. Consequently, optimization efforts to date have relied on Computational Fluid Dynamic (CFD) modeling. Optimization could include adjusting the shape of different AMP components to reduce the cross-sectional area exposed to the strongest currents or incorporating passive farings that reduce form drag by aligning with the direction of the mean currents.

[1]In practice, the dominant length scale for turbulence at tidal current sites is on the order of 10's of meters [7].

B. Methods

Modeling of the AMP and Millennium was performed in SolidWorks (Dessault Systemes SolidWorks Corp., 2012 x64 Edition) and imported into ANSYS Workbench (ANSYS, Inc., Workbench version 14.5) to perform meshing and steady Reynolds Averaged Navier Stokes (RANS) simulations (Fluent). Several other groups have used similar techniques for evaluating ROV and AUV designs [12]–[15]. SolidWorks models of all the instrumentation, AMP support structure,

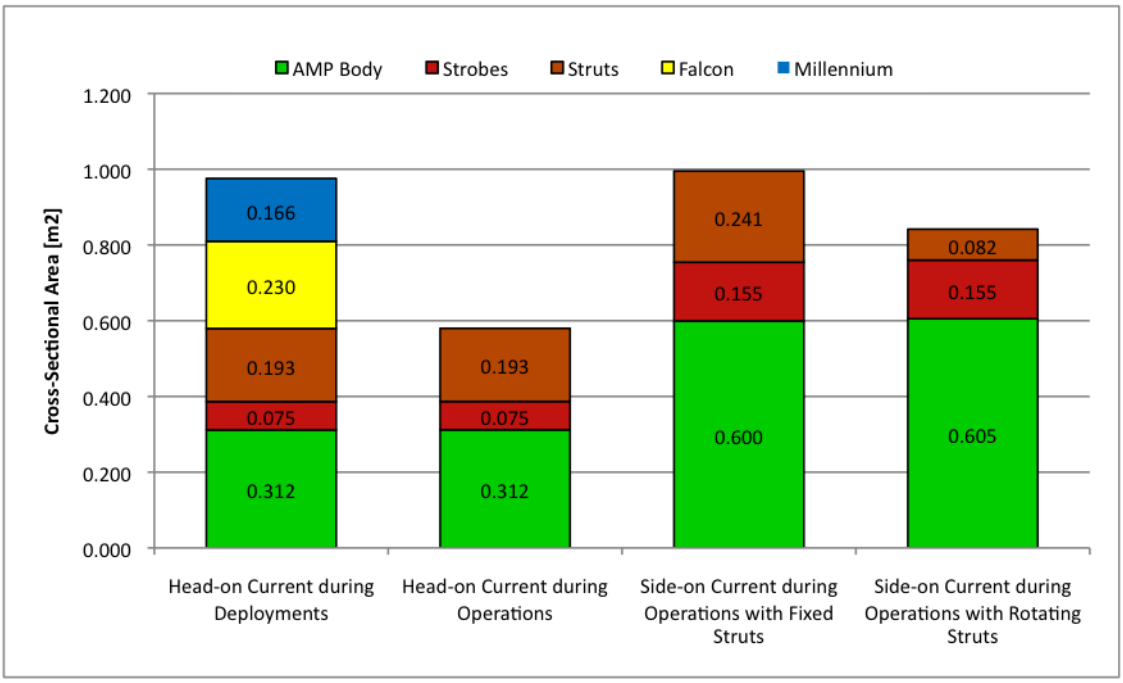

Fig. 5: Component cross-sectional areas for flow simulations

and shroud were used to calculate the center of mass and center of volume, and, therefore, the center of buoyancy. CFD simulations were used to calculate lift and drag coefficients and obtain the center of pressure. The lift and drag coefficients, C_l and C_d, for the various components are calculated as

$$C_l = 2F_l/\rho A U^2 \tag{1}$$

$$C_d = 2F_d/\rho A U^2 \tag{2}$$

where F_l and F_d are the lift and drag forces, ρ is the fluid density, A is the cross sectional area normal to the flow, and U is the mean fluid flow velocity. Cross-sectional areas used in for the calculation of lift and drag coefficients are provided in Fig 5 for each of the simulation models and broken down into the five primary system components shown in Fig. 6a: the Falcon, the Millennium, the central AMP body, the strobes, and the strobe support struts. Fig. 7 illustrates the location and direction of the lift, drag, buoyancy and mass forces in the case of a head–on fluid flow. An analysis of the center of buoyancy, center of pressure, and center of thrust is used to determine the system stability during deployment.

As with all numerical modeling, results should be validated experimentally whenever possible, which will be a focus of future work. For this initial design optimization, the modeling results were used to compare design features and to understand how the drag forces on various components (e.g., strobes, struts, and AMP body) interact when exposed to the design currents. Prior to fabrication of a full-scale AMP prototype, numerical results will be validated through experiments with a sub-scale model in an open channel flume. The full-scale system will then be evaluated in open-water testing and compared to full-scale simulations.

The AMP and Millennium Falcon geometries for the simulations were created in ANSYS DesignModeler from simplified SolidWorks models of the system components. Simplifications were made to the SolidWorks models to prevent meshing errors and reduce computational cost. The mesh was generated in ANSYS Workbench using unstructured tetrahedrons with five inflation layers on all body surfaces. For the flow simulations, the k-ω SST turbulence model was used. This turbulence closure has been shown to predict flow separation better than one-equation closures (e.g., Spalart-Allmaras) or other two-equation closures (e.g., k-ϵ). Drag and lift coefficients were monitored for convergence along with the scaled residuals throughout all simulations. The drag forces acting on the system were monitored for each of the five primary system components shown in Fig. 6a.

Simulations were conducted with mean flow velocities of 0.5, 1.0, and 1.5 m/s to evaluate the sensitivity of the drag coefficient in the expected current range during deployments. Similarly, a grid sensitivity study was performed to determine an appropriate mesh resolution for the CFD analysis of the complete system model shown in Fig. 6a. Three separate meshes were generated from the same geometry by decreasing the minimum element size from an initial setting of 10 mm. Representative meshes are shown in Fig. 8 on the plane of symmetry. The resolution of the 3 meshes that were used is classified as coarse with 1.3 million elements, medium with 2.5 million elements, and fine with 4.9 million elements. While further increases in mesh resolution are possible, decreasing the resolution below 1.3 million elements would actually

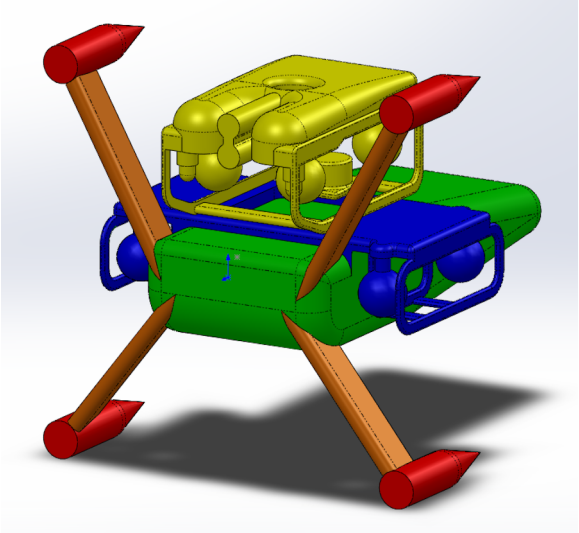

(a) Model used for deployment simulations

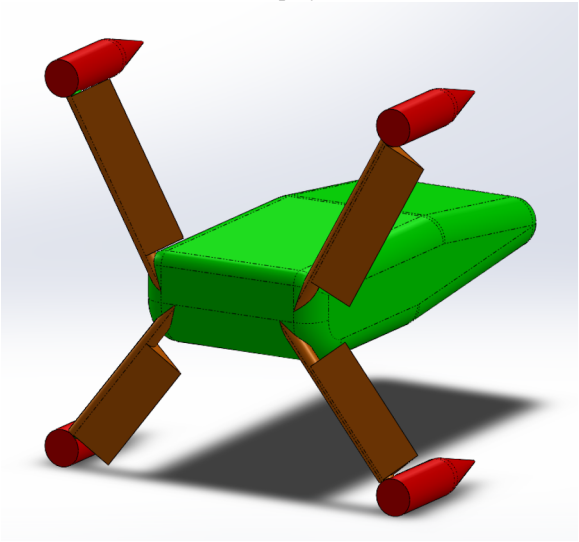

(b) Model with rotated strut farings for side-on current during docked operations

Fig. 6: Simplified AMP and Millennium Falcon geometries for CFD with colors indicating separate components (yellow for Falcon, blue for Millennium, green for AMP body, orange for struts, and red for strobes.)

require significant mesh refinement due to the small features in model.

As a case study for system optimization, CFD simulations were performed for a head-on and side-on flow of the AMP, spanning the range of mounting options during monitoring missions. For the side-on flow case, the faring on the strobe struts was modeled as fixed, as shown in Fig. 6a, or passively aligned with the flow, as in Fig. 6b.

C. Results

Stability of the Millennium Falcon in turbulent currents depends on the balance of forces acting on the system and the

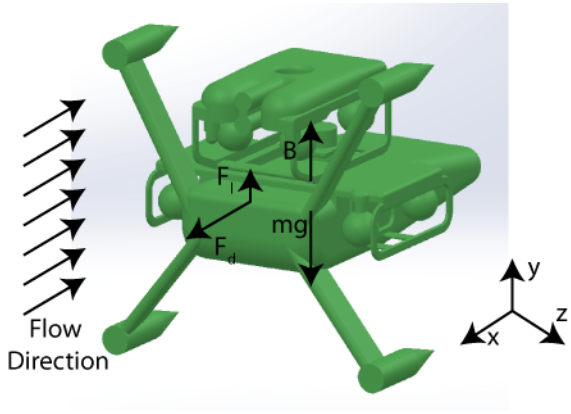

Fig. 7: System free body diagram with approximate locations of lift, drag, buoyancy, and mass forces

TABLE II: Grid dependence of drag coefficient for the Millennium Falcon with the AMP in a head-on mean current of 1 m/s

Grid Sensitivity Study

Mesh Resolution	Coarse Mesh	Medium Mesh	Fine Mesh
Drag Force [N]	316.60	307.75	305.56
Drag Coefficient	0.67	0.65	0.64
% from Coarse Mesh	N/A	2.81%	3.50%

location that those forces are imparted. The righting moment created by the offset of the center of mass and the center of volume will play an important role in minimizing the effect of turbulence. The center of volume of the current design is located 0.693 m behind the frontal plane and 0.022 m above the central axis of the four strobes. By adding ballast to the bottom and floatation to the top of the AMP, the righting moment may be manipulated to allow for increased passive stability. The center of pressure created by the lift and drag forces acting on the model during a head-on flow is located approximately 0.065 m behind the frontal plane and 0.072 m above the central axis. Modest adjustments to the height of the Millennium thrusters will allow the center of thrust to be collocated with the center of pressure to reduce pitching moments during thrusting maneuvers.

CFD visualizations of the normalized flow velocity and total pressure for a 1 m/s head-on mean flow over the Millennium Falcon and AMP are shown in Fig. 9. The flow over the surfaces of the system indicated by the streamlines in Fig.

TABLE III: Velocity dependence of drag coefficient on the Millennium Falcon with the AMP in deployment current range

Velocity Dependence

Flow Velocity [m/s]	0.5	1.0	1.5
Drag Force [N]	79.97	316.60	714.04
Drag Coefficient	0.67	0.67	0.67
% from Coarse Mesh	1.02%	N/A	0.23%

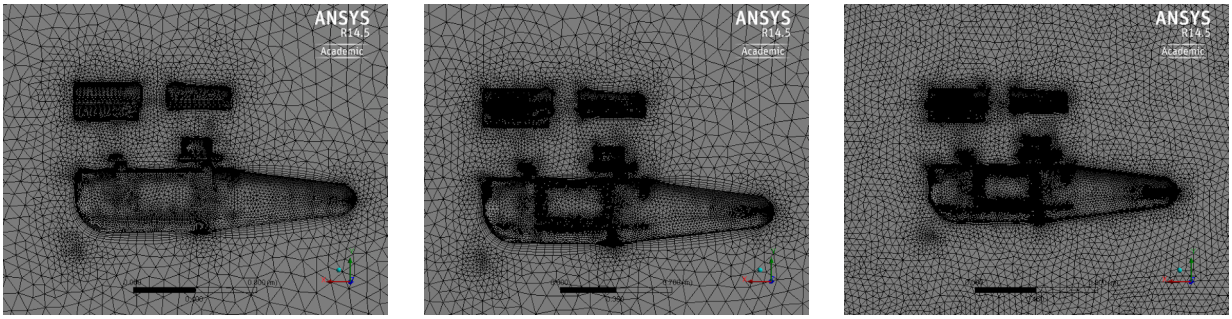

(a) Coarse mesh (b) Medium mesh (c) Fine mesh

Fig. 8: Grid dependence meshing resolutions shown on the axis of symmetry

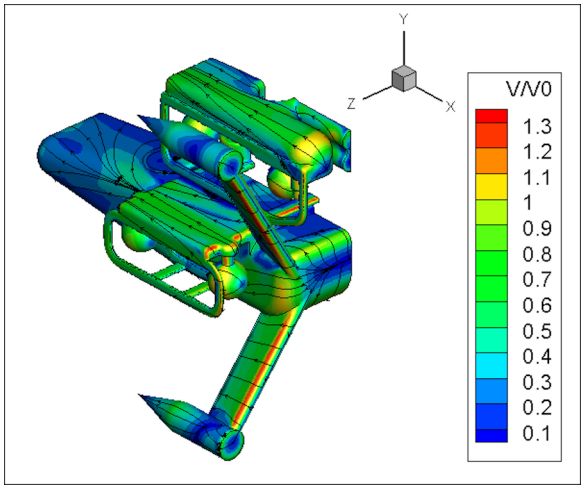

(a) Normalized velocity with streamlines over the body surfaces

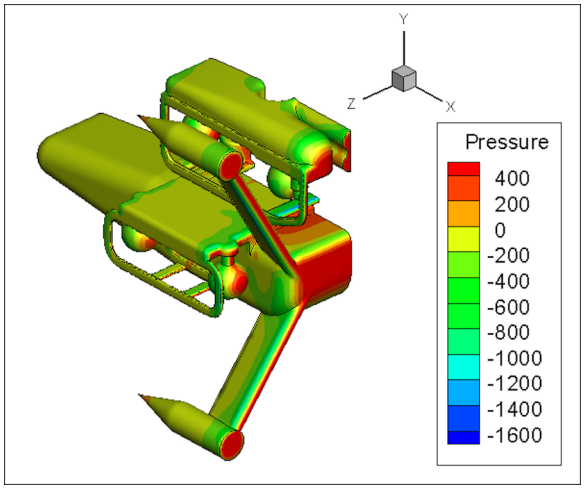

(b) Total pressure [Pa] on the body surfaces

Fig. 9: CFD simulation results for a head-on current of 1 m/s on the Millennium Falcon and AMP

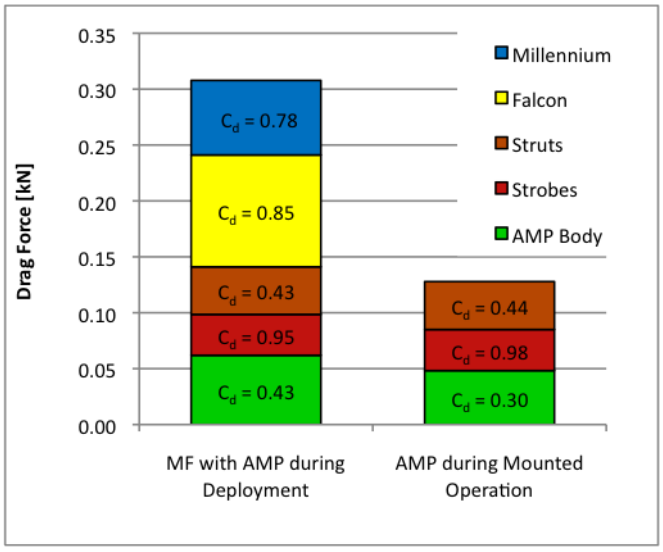

Fig. 10: Drag force and coefficient for the AMP and Millennium Falcon during deployments and mounted operations in a 1 m/s current

9a shows a large eddy forming in the wake of the Millennium Falcon and around the edge of the strobe faces. This flow separation is a significant source of drag on the system due to the added mass effect and will be the focus of future optimizations. Flow over the fared struts, however, shows little to no separation. The high pressure on the frontal faces of the system shown in Fig. 9b indicates the location of form drag which may be reduced through increased faring of these surfaces.

The lift forces calculated in these simulations were negligible and within the range of error since all of the modeled conditions were either a head-on or side-on flow.

The grid sensitivity and velocity dependence studies showed a minimal variation in drag coefficient with differences up to 3.5% from that of the coarse mesh. These results represent the anticipated loading conditions during a deployment and are summarized in Tables II and III for the grid sensitivity and velocity dependence studies respectively. To better understand

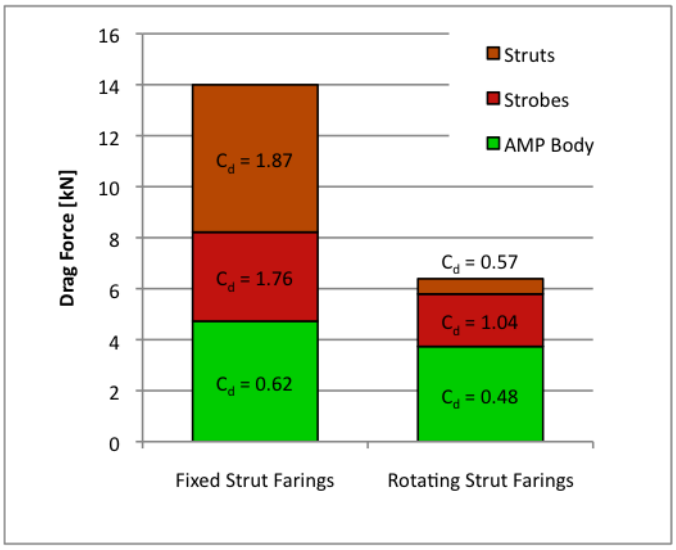

Fig. 11: Drag force and coefficients for a side-on current of 5 m/s over the mounted AMP during operation with fixed or rotating struts

the drag contributions of the individual components, the forces acting on the associated surfaces are shown in Fig. 10 for the AMP in a head-on current of 1 m/s both during deployments with the Millennium Falcon and during mounted operation. It is notable that the draft force on the AMP body is significantly decreased when the Millennium Falcon is disengaged due to the interaction between these sub-systems.

The case study analysis for the AMP during docked operation in 5 m/s currents is summarized in Fig. 11 and indicates a reduction in drag forces of up 54% for the case of side-on current by allowing the strut faring to rotate. Normalized velocity over the AMP bodies for a side-on flow in the negative x direction is visualized in Fig. 12, showing a greater decrease in flow behind the fixed strut faring than the rotating strut faring. The combination of the increased form drag and the increased cross-sectional area of the fixed struts magnifies the drag of this component by 9.6 times when compared to the rotating farings. Similarly to the interaction between the AMP body and the Millennium Falcon, allowing the faring to rotate reduces the drag forces on the strobes and AMP body by reducing blockage at the points where the struts connect.

D. Discussion

The three grid resolutions have limited variation in drag coefficient, suggesting that the numerical solution is grid-independent. Consequently, the coarse grid meshing was used for all subsequent flow simulations to minimize computational cost. Similarly, the velocity sensitivity study suggests that over the range of deployment velocities considered the coefficient of drag is likely to be nearly constant. Additional sensitivity studies addressing the effects of the domain size, meshing elements (regular mesh versus unstructured mesh), and turbulence model will be the subject of future investigation.

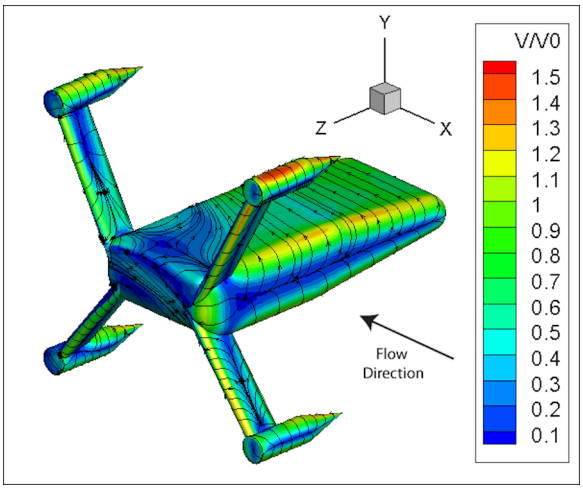

(a) AMP with fixed strut farings

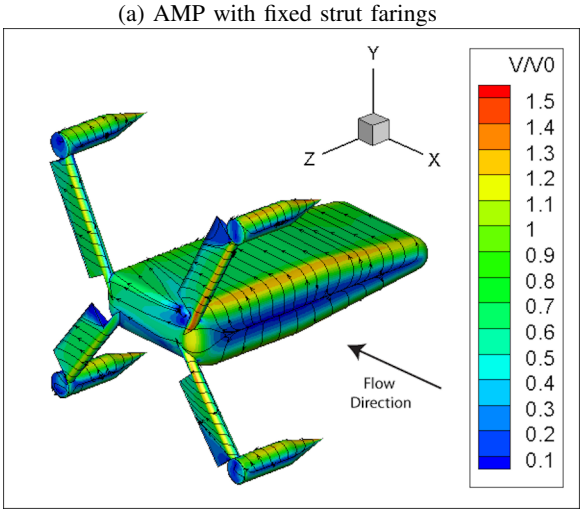

(b) AMP with rotating strut farings

Fig. 12: Optimization case study for a side-on flow over the AMP showing normalized velocity with streamlines

Numerical simulations can assist in optimizing designs without physical prototyping. The case study of the faring on the strobe struts shows that the drag forces on the AMP during docked operation may be reduced up to 54% by allowing the faring to rotate with the current. This reduction is greater than the individual drag contribution of the struts because the drag forces on the AMP body and the strobes are similarly reduced due to interactions between the components. Further improvements in drag reduction using these same methods will be implemented as more details are added to the design.

V. Summary and Next Steps

The design philosophy presented in this paper represents a simple and cost effective means for conducting cabled monitoring in the near–field of wave or tidal energy converters. Integration of a broad and flexible suite of instrumentation into a single shrouded body, such as the AMP, allows the entire monitoring package to be recovered to the surface for

maintenance and reconfiguration. Use of a small inspection class ROV helps to reduce monitoring costs by eliminating the need for a highly specialized support vessel. An initial CFD analysis of this design has provided drag coefficients for the system during deployments and docked operation. With the combined thrust capacity of the Millennium tool skid and the Falcon ROV of 100 kgf and an estimated system drag coefficient of 0.65 for a head-on current during deployments, the maximum current limit will be 1.76 m/s. This significantly exceeds the design goal of 0.7 m/s identified for effective use of the AMP in Admiralty Inlet and provides a margin of thrust for maneuvers in strong currents.

Further optimization of the AMP and Millennium design through the CFD methodology presented here will be the focus of continued efforts on this project over the summer of 2013. The addition of Virtual Blade Models (VBM) to simulate the thrust forces will be used to identify the ideal thruster positions on the Millennium tool skid. Modeling results will be validated through scale-model experimentation in a laboratory flume and open water testing of the full-scale system.

ACKNOWLEDGEMENTS

Funding for this project is provided by the US Department of Energy and Public Utility District No. 1 of Snohomish County. The authors would like to acknowledge a number of helpful discussions on the design of the AMP with David Dyer and Vern Miller at the University of Washington Applied Physics Laboratory, Sean Moran at Oregon State University, Geoff Cook at SeaView Systems, and Danny Miles at Public Utility District No. 1 of Snohomish County, as well as Teymour Javaherchi at the University of Washington for assistance in setting up the numerical simulations of the AMP hydrodynamic performance.

REFERENCES

[1] G. W. Boehlert, G. R. McMurray, and C. E. Tortorici, Eds., *Ecological Effects of Wave Energy Development in the Pacific Northwest*, U.S. Department of Commerce, National Oceanic and Atmospheric Administration, National Marine Fisheries Service. NOAA Technical Memorandum NMFS-F/SPO - 92, September 2008.

[2] G. W. Boehlert and A. B. Gill, "Environmental and ecological effects of ocean renewable energy development," *Oceanography*, vol. 23, no. 2, 2010.

[3] B. Polagye, B. V. Cleve, A. Copping, and K. Kirkendall, Eds., *Environmental effects of tidal energy development*, U.S. Department of Commerce, National Oceanic and Atmospheric Administration, National Marine Fisheries Service. NOAA Technical Memorandum NMFS F/SPO-116, April 2011.

[4] B. Howe and T. McGinnis, "Sensor networks for cabled ocean observatories," in *International Symposium on Underwater Technology*, April 20-23 2004.

[5] A. M. Woodroffe, S. W. Pridie, and G. Druce, "The neptune canada junction box - interfacing science instruments to sub-sea cabled observatories," in *MTS/IEEE Kobe Techno-Ocean*, April 8-11 2008.

[6] A. D. Chave, M. Arrott, C. Farcas, and E. Farcas, "Cyberinfrastructure for the us ocean observatories initiative: Enabling interactive observation in the ocean," in *MTS/IEEE Oceans 2009 - Europe*, May 11-14 2009.

[7] J. Thomson, B. Polagye, V. Durgesh, and M. C. Richmond, "Measurements of turbulence at two tidal energy sites in puget sound, wa," *IEEE Journal of Oceanic Engineering*, vol. 37, no. 3, July 2012.

[8] J. Joslin, B. Polagye, and S. Parker-Stetter, "Development of a stereo camera system for monitoring hydrokinetic turbines," in *Proceedings of the MTS/IEEE Oceans 2012 Conference*. Hampton Roads, VA: MTS/IEEE, October 14-19 2012.

[9] S. M. Wiggins, M. A. McDonald, and J. A. Hildebrand, "Beaked whale and dolphin tracking using a multichannel autonomous acoustic recorder," *The Journal of the Acoustical Society of America*, vol. 131, no. 156, 2012.

[10] J. S. Jaffe, "Underwater optical imaging: the design of optimal systems," *Oceanography*, pp. 40–41, November 1988.

[11] B. Polagye and J. Thomson, "Tidal energy resource characterization: methodology and field study in Admiralty Inlet, Puget Sound, WA (USA)," *Proc. IMechE, Part A: J. Power and Energy*, vol. DOI: 10.1177/0957650912470081, March 22 2013.

[12] J. Long, B. Wu, J. Wu, T. Xiao, and L. Wang, "Estimation of added mass and drag coefficient for a small remotely operated vehicle," in *Proceedings of the 2008 IEEE International Conference on Information and Automation*. Zhangjiajie, China: IEEE, June 20-23 2008.

[13] Y. H. Eng, W. S. Lau, E. Low, G. G. L. Seet, and C. S. Chin, "Estimation of the hydrodynamics coefficients of an rov using free decay pendulum motion," *Engineering Letters*, vol. 16, no. 3, p. 326, 2008.

[14] P. Jagadeesh, K. Murali, and V. Idichandy, "Experimental investigation of hydrodynamic force coefficients over auv hull form," *Ocean Engineering*, vol. 36, pp. 113–118, 2009.

[15] A. M. Dropkin, S. A. Huyer, and C. Henoch, "Combined experimental/numerical development of propulsor evaluation capability," *Journal of Fluids Engineering*, vol. 133, no. 8, p. 081105, 2011.